Elsevier Editorial System(tm) for Planetary and Space Science
Manuscript Draft

Manuscript Number:

Title: Constraints on Jupiter's Stratospheric HCl abundance and chlorine cycle from Herschel/HIFI

Article Type: Research Paper

Keywords: Jupiter; Atmosphere; Composition; Photochemistry; Herschel; sub-millimetre

Corresponding Author: Dr. Nicholas A. Teanby, Ph.D.

Corresponding Author's Institution: University of Bristol

First Author: Nicholas A. Teanby, Ph.D.

Order of Authors: Nicholas A. Teanby, Ph.D.; Adam P Showman, Ph.D.; Leigh N Fletcher, Ph.D.; Patrick G Irwin, Ph.D.

Abstract: Detection of HCl on Jupiter would provide insight into the chlorine cycle and external elemental fluxes on giant planets, yet so far has not been possible. Here we present the most sensitive search for Jupiter's stratospheric HCl to date using observations of the 625.907 and 1876.221 GHz spectral lines with Herschel's HIFI instrument. HCl was not detected, but we determined the most stringent upper limits so far, improving on previous studies by two orders of magnitude. If HCl is assumed to be uniformly mixed, with a constant volume mixing ratio above the 1 mbar pressure level and has zero abundance below, we obtain a 3-sigma upper limit of 0.056 ppb; in contrast, if we assume uniform mixing above the 1~mbar level and allow a non-zero but downward-decreasing abundance from 1~mbar to the troposphere based on eddy diffusion, we obtain a 3-sigma upper limit of 0.024 ppb. This is below the abundance expected for a solar composition source, such as comets, and implies that upper atmosphere HCl loss processes are important. We investigated aerosol scavenging using a simple diffusion model and conclude that it could be a very effective mechanism for HCl removal. Transient scavenging by stratospheric NH3 from impacts is another potentially important loss mechanism. This suggests that it is extremely unlikely that HCl is present in sufficient quantities to be detectable in the near future. We summarise the implications for Jupiter's chlorine cycle and conclude that based on a combination of our observations and previous studies of external oxygen supply, a solar composition external source for Jupiter's chlorine combined with stratospheric scavenging by aerosols and NH3 appears the most plausible.

Highlights (for review)

- HIFI/Herschel observations were used to determine upper limits for HCl on Jupiter
- 3-sigma upper limits are 0.056 ppb (uniform profile) and 0.024 ppb (varying profile)
- Scavenging by stratospheric aerosols could explain the low upper limits
- Results are most consistent with a cometary source for Jupiter's chlorine

Constraints on Jupiter's Stratospheric HCl abundance and chlorine cycle from Herschel/HIFI☆

N. A. Teanby[a], A. P. Showman[b], L. N. Fletcher[c], P. G. J. Irwin[c]

[a]*School of Earth Sciences, University of Bristol, Wills Memorial Building, Queen's Road, Bristol, BS8 1RJ, U.K.*
[b]*Lunar & Planetary Laboratory, University of Arizona, Tucson, Arizona, USA.*
[c]*Atmospheric, Oceanic & Planetary Physics, Department of Physics, University of Oxford, Clarendon Laboratory, Parks Road, Oxford, OX1 3PU. UK.*

Abstract

Detection of HCl on Jupiter would provide insight into the chlorine cycle and external elemental fluxes on giant planets, yet so far has not been possible. Here we present the most sensitive search for Jupiter's stratospheric HCl to date using observations of the 625.907 and 1876.221 GHz spectral lines with Herschel's HIFI instrument. HCl was not detected, but we determined the most stringent upper limits so far, improving on previous studies by two orders of magnitude. If HCl is assumed to be uniformly mixed, with a constant volume mixing ratio above the 1 mbar pressure level and has zero abundance below, we obtain a 3-σ upper limit of 0.056 ppb; in contrast, if we assume uniform mixing above the 1 mbar level and allow a non-zero but downward-decreasing abundance from 1 mbar to the troposphere based on eddy diffusion, we obtain a 3-σ upper limit of 0.024 ppb. This is below the abundance expected for a solar composition source, such as comets, and

☆ *Herschel* is an ESA space observatory with science instruments provided by European-led Principal Investigator consortia and with important participation from NASA.

Email address: n.teanby@bristol.ac.uk (N. A. Teanby)

implies that upper atmosphere HCl loss processes are important. We investigated aerosol scavenging using a simple diffusion model and conclude that it could be a very effective mechanism for HCl removal. Transient scavenging by stratospheric NH_3 from impacts is another potentially important loss mechanism. This suggests that it is extremely unlikely that HCl is present in sufficient quantities to be detectable in the near future. We summarise the implications for Jupiter's chlorine cycle and conclude that based on a combination of our observations and previous studies of external oxygen supply, a solar composition external source for Jupiter's chlorine combined with stratospheric scavenging by aerosols and NH_3 appears the most plausible.

Keywords: Jupiter, Atmosphere, Composition, Photochemistry, Herschel, sub-millimetre

1. Introduction

Detection of HCl provides the potential to reveal unique aspects of chemical, dynamical, and external supply processes on the giant planets. HCl abundance is expected to be extremely variable throughout the atmospheric column and will depend strongly on local atmospheric conditions and the nature of the source reservoir. At the most basic level, Jupiter's bulk chlorine abundance can be estimated from the solar chlorine to hydrogen ratio of 3.2×10^{-6} (Grevesse et al., 2007) combined with the observation that Jupiter is enriched in heavy elements, such as carbon, relative to the solar composition by a factor of about four (Niemann et al., 1998; Wong et al., 2004). If all chlorine is present as HCl and no other processes were occurring, we would expect relative abundances of order 10 ppm based on this argument.

Such high amounts are not present in the observable upper atmosphere and more advanced treatment is required.

Comprehensive thermochemical models of Jupiter's deep interior predict that chlorine is predominantly in the form of HCl (Fegley and Lodders, 1994). However, at pressures less than about 20 bar the temperature drops below 400K and HCl is removed by reaction with tropospheric ammonia (NH_3) to form ammonia salts (NH_4Cl). This reaction is predicted to be extremely fast, so that any HCl dredged up from the deep interior by convection would be immediately removed before it could reach observable atmospheric levels (Fegley and Lodders, 1994; Showman, 2001). Therefore, we do not expect to see any signature from Jupiter's deep HCl reservoir in the stratosphere or upper troposphere.

Another potential source for HCl is externally from comets, interplanetary dust particles, meteoroids, rings particles, or satellites - especially the volcanic moon Io. Observations of trace stratospheric species show the supply of external material to Jupiter's atmosphere is significant (Feuchtgruber et al., 1999; Bézard et al., 2002; Lellouch et al., 2002; Fletcher et al., 2011) and forms an important but poorly understood part of the upper atmosphere chemistry. HCl from external sources would be deposited directly into the stratosphere. Importantly, tropospherically sourced ammonia will have been effectively entirely removed before it reaches the upper stratosphere by a combination of condensation at the tropopause cold trap and photodissociation reactions (Atreya et al., 1977; Atreya and Donahue, 1979). Therefore, externally sourced HCl could avoid removal by reactions with tropospheric ammonia and potentially persist in observable quantities in the upper strato-

sphere and mesosphere (Showman, 2001).

HCl has extremely strong rotational spectral transitions in the far-IR and sub-mm, which when combined with the expectation of potentially significant stratospheric abundances derived from external sources, make it a promising target for spectroscopic detection. Measurements of the amount of HCl in Jupiter's stratosphere would provide constraints on the chlorine cycle and external flux sources and magnitudes. However, despite a long campaign of observations, detection of any halide compound (HCl, HF, HBr, or HI) on any giant planet has remained elusive (Noll, 1996; Weisstein and Serabyn, 1996; Kerola et al., 1997; Fouchet et al., 2004; Teanby et al., 2006; Fletcher et al., 2012). The closest to a positive detection on any of the giant planets was by Weisstein and Serabyn (1996) who produced a tentative detection of 1.1 ppb (parts per billion) HCl on Saturn. However, this was not confirmed by subsequent more sensitive space-based studies, which obtained upper limits of 6.7×10^{-11} (Teanby et al., 2006) and 3.8×10^{-11} (Fletcher et al., 2012) appropriate for the 0.5 bar pressure level. This highlights some of the difficulties of observing halide compounds. The strongest HCl lines occur at frequencies higher than 1 THz, which are not measurable using ground-based telescopes, so weaker lower frequency lines must be used that are susceptible to contamination by telluric water vapour, resulting in much lower sensitivities. Conversely, observations from space-based orbiters tend to have lower spectral resolution and reduced sensitivities to narrow spectral lines.

In the absence of any previous detections of HCl, the external flux of material into Jupiter's atmosphere can be estimated from the observed stratospheric abundances of oxygen species (Feuchtgruber et al., 1997; Feuchtgru-

ber et al., 1999; Bézard et al., 2002), which imply an oxygen flux of 1–4$\times10^6$ atoms/cm^2/s. Assuming a solar relative elemental abundance for Cl/O of 6.9$\times10^{-4}$ (Grevesse et al., 2007) implies a very low external meteoric chlorine (Cl) flux of around 700–2800 atoms/cm^2/s.

However, if instead the dominant contribution to Jupiter's external Cl flux is from Io's plasma torus, which contains a significant amount of chlorine (Küppers and Schneider, 2000). Showman (2001) estimates that the total chlorine flux could be much higher: 3×10^6 atoms/cm^2/s if all of Io's torus material eventually enters Jupiter's atmosphere; or a more reasonable 7×10^4 atoms/cm^2/s for an entry fraction based on the measured Cl/O ratios and external oxygen flux. Showman (2001) used the latter Cl flux with a 1D diffusion-transport model to predict a maximum abundance of HCl in Jupiter's stratosphere. At the 1 mbar pressure level the model predicted 1 ppb HCl in Jupiter's upper stratosphere, with a sharp decrease in abundance with increasing pressures caused by vertical mixing. The modelled profile is most appropriate for the stratosphere as there is expected to be significant scavenging from ammonia in the troposphere which was not included in the diffusion profile calculation. However, for the purpose of comparison with previously published upper limits, the model can be used to predict an upper bound on externally sourced HCl at around 0.5 bar of $\sim3\times10^{-13}$ for Jupiter and $\sim10^{-13}$ for Saturn. The model predictions are consistent with the most stringent current upper limits for HCl in Jupiter's troposphere of 2.3 ppb derived by Fouchet et al. (2004) using Cassini's CIRS instrument (Flasar et al., 2004). The predictions are also consistent with upper limits derived for Saturn of 6.7×10^{-11} determined by Teanby et al. (2006) using CIRS

and 3.8×10^{-11} determined by Fletcher et al. (2012) using Herschel/SPIRE. Therefore, further constraints on the vertical distribution require orders of magnitude more sensitivity than previous measurements.

The Herschel space telescope was specifically designed to observe the sub-mm spectral region and is ideally suited to a search for HCl, which should be easily detectible on Jupiter if it is present in ∼ppb quantities at 1 mbar. Herschel's Heterodyne Instrument for the Far-Infrared (HIFI) (de Graauw et al., 2010) provides the best opportunity to accurately measure Jupiter's stratospheric HCl for the foreseeable future, which motivates the present study; there are no spacecraft with suitable remote sensing instruments scheduled to visit Jupiter, or any other giant planet, for the next two decades at least. HIFI's low noise and high spectral resolution means that our observations will be sensitive to parts per trillion HCl levels - an improvement of around two orders of magnitude on the best measurements currently available (Fouchet et al., 2004). This allows us to place new constraints on Jupiter's chlorine cycle.

2. Observations

Our HIFI observations were proposed as part of Herschel's OT1 call in 2010 (program ID: `OT1_nteanby_2`) and were observed on 28$^{\text{th}}$ February and 7$^{\text{th}}$ March 2013 (just under two months before the coolant ran out on 29$^{\text{th}}$ April 2013). We focused on the two HCl rotational bands that had the maximum predicted signal-to-noise: 625.907 GHz in band 1; and 1876.221 GHz in band 7. Predicted signals were 0.082K at 625.907 GHz and 2.1K at 1876.221 GHz assuming an effective spectral resolution of 10 MHz

and an abundance profile with 1 ppb HCl for pressures less than 1 mbar. We determined integration times using Herschel's HSpot observation tool by aiming for a high overall signal-to-noise ratio (S/N) of ∼100 to allow for the large uncertainties in HCl abundance. For band 1, total integration time was 13600 seconds, split over three separate observations with a predicted overall instrument noise level of 0.0012K per 10.5 MHz bandwidth and a S/N of 70. For band 7, total integration time was 8742 seconds, again split over three separate observations with a predicted overall instrument noise level of 0.016K per 10.5 MHz bandwidth and a S/N of 130.

Observations were taken in HIFI's dual beam switch single point observation mode (HIFI Observers' Manual, 2011), which resulted in maximum efficiency within time allocation constraints. Both wide band spectrometer (WBS) and high resolution spectrometer (HRS) were used, with resolutions of 1.1 MHz and 0.25 MHz respectively. The WBS and HRS had the same sensitivity for a given frequency interval, so the HRS data was only recorded to provide information on the vertical profile of HCl in the case of a detection. As HCl was not detected we only consider the WBS measurements here. Local oscillator frequencies of 620.303 GHz and 1873.233 GHz were used and both upper and lower sidebands were measured. However, only the upper side band is considered here as that contains the HCl lines; as expected no other spectral features were observed in either side band. Horizontal and vertical polarisations were measured separately. The WBS had a band width of 4 GHz in band 1 and 2.4 GHz in band 7.

Observations had a single on-planet pointing centred on Jupiter, which had an angular diameter of approximately 39". Herschel's 3.28 m primary

mirror had Airy disc sizes of 36.7" and 12.3" in bands 1 and 7 respectively, which resulted in disc-averaged spectra for band 1 and a low spatial resolution disc-centred average for band 7; the effect of this on the observed spectra is considered further in section 3.2. Full observation details are summarised in Table 1.

3. Data reduction

3.1. Level 2 data products

Data were first processed using v10 of the standard HIPE pipeline (Ott, 2010) to give calibrated antenna temperatures T_a in both upper and lower sidebands for each observation. Figure 1 shows the Level 2 post-pipeline calibrated data, from which it is immediately obvious that the spectra were affected by instrumental standing waves and long-period continuum ripples with amplitudes of up to 4 K; much higher than the intrinsic instrument noise. These standing waves are due to reflections within the instrument, which result in quasi-sinusoidal interference with approximate periods of 92, 98, 100, and 320 MHz in bands 1 and 7 (Roelfsema et al., 2012). band 1 is most affected by the 100 MHz standing waves, whereas band 7 is most affected by the 320 MHz standing waves. Therefore, more advanced processing was required before any useful information on HCl could be obtained.

3.2. HCl lineshape

Before performing any additional processing on the data, we first consider the predicted signal in more detail and determine the exact shape of the HCl emission lines, as this determines the level of standing wave removal that can

be achieved. If HCl can be assumed to exist above 1 mbar only, then the resulting emission lines should be very narrow, with widths of <10 MHz. Such narrow lines could be easily separated from the 100 MHz standing waves. However, because of the large field-of-view and rapid rotation of Jupiter, the major contribution to the effective observed line width is rotationally induced doppler broadening. To calculate the line profile due to doppler broadening we generated a synthetic image of Jupiter with 2001×2001 pixels, and for each pixel calculated the emission angle, line-of-sight velocity, and associated doppler shift. Each pixel was then weighted using Herschel's Airy disc and the overall effective lineshape constructed from the weighted average contribution from each pixel to the disc-averaged spectrum. A weighted mean emission angle for each band was also calculated from the pixel map for use in the radiative transfer modelling in section 4. Figure 2 shows the calculated lineshapes for bands 1 and 7, which have full-width half maximum (FWHM) of 35.39 MHz and 39.65 MHz respectively.

3.3. Minimisation of standing wave interference

By an unfortunate coincidence, Jupiter's rotation rate is such that the FWHMs of the effective lineshapes are comparable to the FWHMs of the 92, 98, and 100 MHz instrumental standing waves (30.6, 32.7, and 33.3 MHz respectively). This means that the standard HIPE baseline remove methods could not be used without compromising the signal. Therefore, we developed our own post-processing algorithm, taking great care not to adversely affect any potential HCl signature. First, for each band, the six individual spectra (3 x 2 polarisations) were high-pass filtered using a 4 pole Butterworth filter (Gubbins, 2004) with a corner period of 200 MHz. This effectively

suppressed the 320 MHz standing waves and any long period continuum offsets, resulting in spectra of antenna temperature difference ΔT_a relative to the baseline/continuum level. Second, for each band, the six spectra were binned and averaged with a bin width of 9 MHz to reduce the random noise. Any emission lines present would be much wider than these bins and would not be affected. Antenna temperature errors in each bin were calculated from the unweighted standard error of the six individual spectra. Third, a masked spectrum was produced by removing datapoints within $\pm$30 MHz of the HCl spectral lines in band 1 and $\pm$40 MHz of the the HCl spectral lines in band 7. This left spectra that were assumed to be composed entirely of standing waves and random noise (there are no other known gas lines in this range). Fourth, a least squares minimisation method was used to fit a single period sine wave to each of the masked spectra. The standing waves were not well represented by a single sine wave over the entire bandwidth, due to their quasi-sinusoidal nature, so the range fitted was limited to 2.2 GHz in band 1 and 1.5 GHz in band 7, which gave good fits around the predicted positions of the HCl features. The fitted sine waves were assumed to represent the standing wave component and were removed from the binned spectra. These final processed spectra were converted from an antenna temperature difference ΔT_a into a main beam temperature difference ΔT_{mb} using:

$$\Delta T_{mb} = \Delta T_a \frac{\nu_l}{\nu_{mb}} \tag{1}$$

where ν_l is the forward efficiency and ν_{mb} is the main beam efficiency (Wilson et al., 2009; HIFI Observers' Manual, 2011). Instrument calibration gives $\nu_l = 0.96$, $\nu_{mb} = 0.76$ in band 1, and $\nu_{mb} = 0.69$ in band 7 (Roelfsema et al., 2012). To determine the brightness temperature difference ΔT_b, ΔT_{mb} was

divided by a fill factor s, which is the response weighted area of Jupiter that intersects the main beam divided by the response weighted area of the main beam. The values of s were 0.75 for band 1 and 1.00 for band 7. These data processing stages are illustrated in Figure 3. The final noise levels were about 0.05–0.1K in both bands. While this method gives and order of magnitude improvement in the noise over the standard pipeline product, the noise levels are still higher than those predicted using HSpot by a factor of 40–80 for band 1 and 3–6 for band 7. Band 1 is severely affected by $\sim$100 MHz standing waves, whereas the 320 MHz standing waves which are more prevalent in band 7 are more easily removed. The HCl emission lines are also much stronger in band 7, meaning that band 7 provides by far the most powerful constraint on Jupiter's HCl.

4. Spectral modelling

The change in brightness temperature due to HCl was calculated using the NEMESIS radiative transfer code (Irwin et al., 2008). This has been used extensively on Jupiter in the past (e.g. Fletcher et al., 2009; Nixon et al., 2010). We assumed a globally homogeneous vertical atmospheric structure using the temperature profile from Seiff et al. (1996). NH_3, PH_3, and CH_4 profiles were based on Fletcher et al. (2009), although these gases only contribute minimally to the continuum in our spectral regions. H_2 and He abundances were derived from Galileo probe measurements (Niemann et al., 1998). We assumed equilibrium para-H_2 fraction throughout the atmosphere. Aerosols have negligible opacity in the sub-mm and were not included in our atmospheric model.

Collision induced absorption due to H_2-H_2, H_2-He, H_2-CH_4, and He-CH_4 pairs were included according to the formulations in Borysow et al. (1985, 1988); Borysow and Frommhold (1986, 1987); and Borysow (1991). Spectroscopic data were taken from HITRAN2004 (Rothman et al., 2005). NEMESIS uses the correlated-k approximation to calculate atmospheric opacity (Goody and Yung, 1989; Lacis and Oinas, 1991), so we incorporated the doppler lineshapes from section 3.2 directly into the k-tables for computational efficiency. The emission angle was assumed to be the Airy-weighted disc-averaged emission angle from section 3.2.

We considered two end member HCl reference profiles: the first had constant volume mixing ratio HCl for pressures lower than 1 mbar, and zero HCl at higher pressures (subsequently referred to as [1 mbar]); and the second was the profile given by the 1D diffusion model from Showman (2001) (subsequently referred to as [S01]). Each reference profile had HCl set to a uniform 1 ppb for all pressures less than 1 mbar. The [S01] 1D diffusion profile is appropriate for an external source at or above the 1 mbar pressure level with no HCl loss processes other than dilution with the bulk atmosphere due to eddy mixing. Conversely, the [1 mbar] profile is appropriate if HCl loss processes are significant in the middle stratosphere. Figure 4 shows the assumed temperature profile, reference HCl profiles, contribution functions, and corresponding synthetic spectra.

5. HCl upper limits

To calculate upper limits for HCl we follow a forward modelling approach similar to Teanby et al. (2013) and Teanby and Irwin (2013). Reference pro-

files were scaled, then used to calculate synthetic spectra, which were compared to the observations. For a given 1 mbar HCl abundance α we calculate the misfit $\chi^2(\alpha)$ between the measured brightness temperature difference spectra $y_i \pm \sigma_i$ and a synthetic brightness temperature difference spectrum $f_i(\alpha)$:

$$\chi^2(\alpha) \;=\; \sum_{i=1}^{n} \frac{\left(y_i - f_i(\alpha)\right)^2}{\sigma_i^2} \qquad (2)$$

where both measured and synthetic spectra are defined at n frequencies ν_i with $i = 1 \ldots n$. The best fitting HCl abundance $\alpha_{\rm opt}$ is where $\chi^2(\alpha)$ is minimised. There is one free parameter (α), so for the abundance to be significant at the 3-σ level $\Delta\chi^2 = \chi^2(\alpha_{\rm opt}) - \chi^2(0)$ must be less than -9 (Press et al., 1992). In the case of no significant minimum, the 3-σ upper limit is given by the value of α where $\Delta\chi^2 = +9$.

Figure 5 shows the variation of χ^2 as a function of 1 mbar HCl abundance derived from scaling each of the two reference profiles, for band 1 and band 7. No significant minima are present, indicating that we can only derive upper limits from these data. Band 1 and band 7 data are consistent with each other, but overall band 7 provides the most stringent constraint on Jupiter's stratospheric HCl. The 3-σ upper limits on HCl abundance at 1 mbar are: 0.024 ppb when scaling the [S01] profile; and 0.056 ppb when using the [1 mbar] profile. Figure 6 shows the measured spectra along with a 3-σ synthetics for comparison.

6. Discussion

6.1. Possible external sources of chlorine

We can gain insight into potential sources of chlorine by combining our HCl upper limits with the derived oxygen flux into Jupiter, which has the advantage that oxygen species have actually been detected so are far better constrained. Bézard et al. (2002) and Lellouch et al. (2002) show that most of Jupiter's stratospheric oxygen is in the form of CO, H_2O, or CO_2. These species have strong vertical gradients in the stratosphere consistent with an external source. Potential oxygen sources include interplanetary dust particles, micrometeorites, comets, and Io's plasma torus. Most of Jupiter's stratospheric oxygen is in the form of CO. This is unusual, given that H_2O should be more abundant in interplanetary dust particles (IDPs), micrometeorites, and comets and suggests that shock chemistry during large impacts is required to convert H_2O to CO (Bézard et al., 2002). IDPs and micrometeorite impacts would not produce enough energy to convert H_2O to CO so 0.3–1.6 km sized comet impacts are preferred by Bézard et al. (2002). The CO production rate required to explain Bézard et al. (2002)'s observations is 4×10^6 molecules/cm^2/s and is the dominant production rate of any oxygen species in the upper atmosphere. Therefore, we can constrain the total oxygen influx (initially in either CO or H_2O molecular form) to also be 4×10^6 molecules/cm^2/s. We now use this flux to predict chlorine flux for different source assumptions:

- If the chlorine source is from comets, a solar Cl/O ratio of 6.9×10^{-4} is reasonable (Grevesse et al., 2007), implying a chlorine flux of 2.8×10^3 molecules/cm^2/s. IDPs and micrometeorites can be discounted

as they would not result in sufficient CO production, but would also provide a similar chlorine flux.

- If both the oxygen and the chlorine source is Io's plasma torus, we can use the observed Cl/O ration from Küppers and Schneider (2000) of 1/15 to derive a chlorine flux of 2.7×10^5 molecules/cm^2/s - around 100 times that expected from comets. This flux would correspond to about 10% of Io's plasma torus eventually entering Jupiter's atmosphere. This scenario seems unlikely given the shock chemistry arguments required to explain the oxygen species, but is considered for completeness.

These predictions can now be compared to our HCl upper limits using a numerical 1D diffusion model with and without loss processes.

6.2. Diffusion model HCl profile predictions with no loss

We start by assuming that all external chlorine forms HCl and the only process operating is dilution with a HCl-free bulk troposphere via eddy mixing. We then formulated a numerical 1D diffusion model by adapting the analytical model outlined in Showman (2001). Briefly, we split the atmosphere into N layers of equal thickness Δz with altitudes z_i where $i = 1 \ldots N$ covering pressures from 10 bar to 1 mbar. The upward flux of HCl was determined using:

$$\phi(z) = -K(z) \left[\frac{dn(z)}{dz} + \frac{n(z)}{H(z)} + \frac{n(z)}{T(z)} \left(\frac{dT(z)}{dz} \right) \right] \quad (3)$$

where $K(z)$ is the eddy diffusion coefficient, $n(z)$ is the number density of HCl, $H(z)$ is the atmospheric scale height (RT/Mg), and $T(z)$ is the temperature (Showman, 2001; Chamberlain and Hunten, 1987). The bottom

boundary condition was defined by:

$$n(z_1) \;=\; \frac{\phi(z_1)H(z_1)}{K(z_1)} \tag{4}$$

The HCl profile was then calculated using a finite-difference time-stepping approach in which the change in HCl number density at each level z_j in time Δt was given by the approximation:

$$\Delta n(z_j) \;=\; \frac{(\phi(z_{j-1}) - \phi(z_{j+1}))}{2\Delta z}\Delta t \tag{5}$$

We set an input flux of $-\phi_0$ at the model top, where ϕ_0 is the (downward) input flux from our source scenario. For the first time step, $n(z)$ is initialised to zero at all levels except for the top level, which has $n(z_N) = -\phi_0 \Delta t/\Delta z$. The model was then iterated for 1000 model years with 1hr time steps to determine the steady state HCl profile, which is independent of the initial HCl profile. This numerical model reproduces the analytical solution presented in Showman (2001) under equivalent assumptions, but provides the additional flexibility needed to include loss processes.

Figure 7 shows the model parameters and predicted HCl profiles for input HCl fluxes of 2.8×10^3 and 2.7×10^5 molecules/cm^2/s. These profiles are effectively scaled versions of each other; as we have not yet included any loss processes, the HCl abundance at each level is simply a function of the input flux and the eddy diffusion. The model predicts HCl abundances at 1 mbar of 0.05 ppb (for 2.8×10^3 molecules/cm^2/s from comets) and 5 ppb (for 2.7×10^5 molecules/cm^2/s from Io). These can be considered maximum values as loss has been neglected and also because not all externally supplied Cl will be in form of HCl. Recent observations of comet Hartley 2 (Bockelée-Morvan et al., 2014) suggest HCl is sub-solar in comets and chlorine could

hence be in other forms. However, it is reasonable to assume that reduction in Jupiter's hydrogen-rich upper atmosphere would lead to creation of HCl, at least initially.

If loss processes in the upper stratosphere can be ignored, our upper limits are most consistent with the lower Cl flux predicted by an approximately solar composition external source. If Io were the source, at least 200 times more HCl would be expected than our observations suggest. However, even a solar composition external source predicts too much HCl - 0.05 ppb compared to our upper limit of 0.024 ppb. This suggests HCl loss processes are important in Jupiter's upper stratosphere and cannot be ignored.

6.3. Diffusion model HCl profile predictions with aerosol scavenging

Our modelling suggests that stratospheric HCl loss processes must be considered in order to explain the very low upper limits. Therefore, we now consider the effect of potential loss mechanisms for HCl in the stratosphere. Scavenging by stratospheric aerosols could be a significant sink of HCl. To model this we first define an accommodation coefficient, γ, which is the fraction of HCl-aerosol collisions that result in HCl sticking to the aerosol and being scavenged. This parameter is poorly constrained and will depend on the precise composition and physical structure of the aerosol, so we treat it as a free parameter in the model. Values of γ in the range 0.1–1 seem reasonable based terrestrial scavenging processes (Tabazadeh and Turco, 1993; Davis, 2006), especially for droplets of water (Schweitzer et al., 2000), impure water solutions (Li et al., 2002; Rudich, 2003) or ammonia (see discussion in Showman, 2001). However, such droplets are unlikely to be representative of Jupiter's upper stratosphere aerosols, which are most likely to be based

on photochemically produced hydrocarbons. Experiments on organic compounds suggest γ could be much lower; perhaps as low as 0.001–0.01 (Zhang et al., 2003) for experiments with octanol. It is possible that values of γ for scavenging by Jupiter's aerosols could be even lower. Therefore, to cover the large uncertainty, we consider γ's in the range 10^{-5}–1.0 as well as $\gamma = 0$, which represents no loss.

To determine the number of HCl-aerosol collisions, we also require the aerosol properties, specifically their number density and radii as a function of altitude. These are also poorly constrained in the upper stratosphere, so we use the values from the model of Banfield et al. (1998) to estimate the magnitude of the scavenging effect. This model includes aerosol growth during descent through the atmosphere.

To determine collision rates, consider an ideal gas containing HCl molecules and aerosol particles. From gas kinetic theory (e.g. Tabor, 1993; Woan, 2003), the mean speed $\overline{c}$ of the HCl molecules is given by:

$$\overline{c} = \left(\frac{8kT(z)}{\pi m} \right)^{1/2} \tag{6}$$

where k is the Boltzmann constant and m is the mass of one HCl molecule, resulting in typical speeds of 310 ms^{-1} at 1 mbar in Jupiter's upper stratosphere. The aerosol particles, being relatively heavy, can be assumed to be effectively stationary with respect to the rapidly moving HCl molecules. The aerosol particles have a relatively large radius r_a of order 0.1 μm, so the HCl molecules can be assumed to have negligible radius. This implies that a HCl-aerosol collision will occur if a HCl molecule comes within r_a of an aerosol particle. Therefore, in time t a single HCl molecule sweeps out a potential collision volume $V = \pi r_a^2 \overline{c} t$. If the number density of aerosol particles is n_a,

this results in $\pi r_a^2 \overline{c} n_a$ collisions per second, with an average time between collisions of $\delta t = 1/\pi r_a^2 \overline{c} n_a$. The probability $P(x)$ of a HCl molecule not colliding with an aerosol particle is given by the survival equation:

$$P(x) = \exp(-x/\lambda) \quad (7)$$

where $x = \overline{c}\Delta t$ is the distance travelled in each time step and $\lambda = \overline{c}\delta t$ is the mean free path (Tabor, 1993). If a fraction γ of collisions result in scavenging of the HCl molecule by the aerosol particle, the probability $P'(t)$ of a HCl molecule being scavenged in time t is:

$$P'(t) = \gamma(1 - \exp(-t/\delta t)) \quad (8)$$

So after each time step Δt, the fraction of HCl remaining $R(\Delta t)$ is given by:

$$R(\Delta t) = 1 - \gamma(1 - \exp(-\pi r_a^2 \overline{c} n_a \Delta t)) \quad (9)$$

This loss process was applied to the HCl number density $n(z)$ after each time step in our diffusion model.

Figure 7 shows the resulting HCl profiles for HCl injection at 1 mbar and a reasonable range of values for γ. Unless HCl-aerosol collisions are extremely inefficient at scavenging, HCl is removed very quickly and cannot build up in observable quantities. If we assume aerosol scavenging is the sole loss process, our upper limits can be used to place moderate constraints on the chlorine source. For an Io based chlorine source, γ must be greater than 0.1 to be consistent with our upper limits, whereas for solar composition source γ need only be greater than 10^{-5}. Based on the literature, low values of γ appear more likely for organic aerosols, which argues for a solar composition source. However, there are many uncertainties in our model, for example,

if HCl injection is higher in the atmosphere then scavenging could be even more efficient due to the greater combined surface area of smaller aerosol particles at higher altitudes.

Additional complications arise because aerosol scavenging is not the only possible loss process: reactions with ammonia is another potential mechanism. Scavenging by tropospheric NH_3 was considered in detail by Showman (2001) and is not considered further here. We consider this to be a minor process as most NH_3 is removed by cold trap, and any small residual would be destroyed by photolysis well below 1 mbar pressure level (Atreya et al., 1977; Atreya and Donahue, 1979). The effectiveness of NH_3 destruction in the atmosphere by photolysis is very efficient, as evidenced by the rapid depletion in NH_3 injected by the SL9 impact (Fast et al., 2002; Moses et al., 1995). Perhaps more important than tropospherically sourced NH_3 is periodic NH_3 injection by cometary impacts, which can provide significant transient NH_3 abundances at these altitudes, reaching >1 ppm over local scales (Fast et al., 2002). Cometary impacts that penetrate deeper into the atmosphere may also excavate tropospheric NH_3 into the stratosphere via entrainment in impact plumes (Fletcher et al., 2011). Such transient NH_3 sources could easily remove ppb amounts of HCl by formation and subsequent precipitation of NH_4Cl salts.

Our extremely low HCl upper limits are suggestive of, and consistent with, the estimated high efficiency of scavenging processes in Jupiter's upper stratosphere; either by aerosols or transient NH_3 from comet impacts. Unfortunately, in the presence of such scavenging, we cannot unambiguously distinguish between potential HCl sources, as both Io's plasma torus and

cometary input fluxes could be removed efficiently enough to prevent a detection with Herschel. However, our observations and modelling are most consistent with a cometary source for the supply of external material into Jupiter's upper atmosphere.

Figure 8 schematically summarises the implications of our observations and modelling, combined with those from previous studies, for Jupiter's chlorine cycle.

7. Conclusion

We used Herschel's HIFI spectrometer to derive stringent new upper limits for HCl in Jupiter's atmosphere. For a profile that has constant HCl above the 1 mbar level we obtain a 3-σ upper limit of 0.056 ppb, whereas scaling a 1D diffusion model based profile with an upper atmosphere source gives a 3-σ upper limit of 0.024 ppb. Therefore, if HCl is present in Jupiter's upper atmosphere it must be in extremely small amounts. For comparison, the previous best upper limit was 2.3 ppb (Fouchet et al., 2004) at around 0.5 bar. Our lossless diffusion model combined with a source with solar Cl/O relative abundances would predict abundances of $\sim$0.05 ppb at the 1 mbar pressure level and $\sim$1–2$\times10^{-14}$ at the 0.5 bar pressure level.

If HCl scavenging by stratospheric aerosols or ammonia is negligible, our upper limits rule out Io's plasma torus as a source for chlorine and are more consistent with a source with a lower, approximately solar, Cl/O ratio such as comets. However, our HCl upper limit is lower than the abundance predicted by such a source, which suggests that HCl scavenging of some kind is indeed occurring. Therefore, based on this and on our modelling, negligible loss of

HCl in the upper stratosphere seems highly unlikely.

Our modelling suggests that scavenging by stratospheric aerosols is likely to be a significant loss process, and is very efficient for reasonable aerosol number densities and accommodation coefficients. In the steady state atmosphere, scavenging of HCl by internally sourced NH_3 is unlikely as it would be destroyed by photolysis at much lower altitudes. However, NH_3 transients caused by cometary impacts such as SL9 could be a very efficient further loss mechanism, either by direct NH_3 injection or by dredging up deep NH_3 by entrainment of tropospheric material in impact plumes. The efficiency of potential loss mechanisms limits our ability to constrain the source of Jupiter's chlorine flux. However, our results favour a solar composition source (such as comets) because less extreme aerosol accommodation coefficients are required.

Further constraints on Jupiter's chlorine cycle would require laboratory measurements of HCl accommodation coefficients and better quantification of upper stratospheric aerosols. Direct detection of HCl would require an increase in sensitivity of many orders of magnitude and seems unrealisable given current technology.

8. Acknowledgements

This work was funded by the UK Science and Technology Facilities Council, the Leverhulme Trust, the NASA Planetary Atmospheres Program, and the Royal Society. The authors would like to thank Mark Kidger, David Teyssier, and Anthony Marston at the Herschel Science Centre for help with observation planning and design. HIFI has been designed and built by a

consortium of institutes and university departments from across Europe, Canada and the United States under the leadership of SRON Netherlands Institute for Space Research, Groningen, The Netherlands and with major contributions from Germany, France and the US. Consortium members are: Canada: CSA, U.Waterloo; France: CESR, LAB, LERMA, IRAM; Germany: KOSMA, MPIfR, MPS; Ireland, NUI Maynooth; Italy: ASI, IFSI-INAF, Osservatorio Astrofisico di Arcetri-INAF; Netherlands: SRON, TUD; Poland: CAMK, CBK; Spain: Observatorio Astronmico Nacional (IGN), Centro de Astrobiologa (CSIC-INTA). Sweden: Chalmers University of Technology - MC2, RSS & GARD; Onsala Space Observatory; Swedish National Space Board, Stockholm University - Stockholm Observatory; Switzerland: ETH Zurich, FHNW; USA: Caltech, JPL, NHSC. HCSS / HSpot / HIPE is a joint development (are joint developments) by the Herschel Science Ground Segment Consortium, consisting of ESA, the NASA Herschel Science Center, and the HIFI, PACS and SPIRE consortia.

References

Atreya, S.K., Donahue, T.M., 1979. Models of the Jovian Upper Atmosphere. Rev. Geophys. & Space Phys. 17, 388–396.

Atreya, S.K., Donahue, T.M., Kuhn, W.R., 1977. The distribution of ammonia and its photochemical products on Jupiter. Icarus 31, 348–355.

Banfield, D., Conrath, B.J., Gierasch, P.J., Nicholson, P.D., Matthews, K., 1998. Near-IR Spectrophotometry of Jovian aerosols - meridional and vertical distributions. Icarus 134, 11–23.

Bézard, B., Lellouch, E., Strobel, D., Maillard, J.P., Drossart, P., 2002. Carbon Monoxide on Jupiter: Evidence for Both Internal and External Sources. Icarus 159, 95–111.

Bockelée-Morvan, D., Biver, N., Crovisier, J., Lis, D.C., Hartogh, P., Moreno, R., de Val-Borro, M., Blake, G.A., Szutowicz, S., Boissier, J., Cernicharo, J., Charnley, S.B., Combi, M., Cordiner, M.A., de Graauw, T., Encrenaz, P., Jarchow, C., Kidger, M., Küppers, M., Milam, S.N., Müller, H.S.P., Phillips, T.G., Rengel, M., 2014. Searches for HCl and HF in comets 103P/Hartley 2 and C/2009 P1 (Garradd) with the Herschel Space Observatory. Astron. Astrophys. 562, A5. 1401.1104.

Borysow, A., 1991. Modelling of collision-induced infrared-absorption spectra of H_2-H_2 pairs in the fundamental band at temperatures from 20K to 300K. Icarus 92, 273–279.

Borysow, A., Frommhold, L., 1986. Theoretical collision-induced rototranslational absorption spectra for the outer planets: H_2-CH_4 pairs. Astrophys. J. 304, 849–865.

Borysow, A., Frommhold, L., 1987. Collision-induced rototranslational absorption spectra of CH_4-CH_4 pairs at temperatures from 50 to 300K. Astrophys. J. 318, 940–943.

Borysow, J., Frommhold, L., Birnbaum, G., 1988. Collision-induced rototranslational absorption-spectra of H_2-He pairs at temperatures from 40 to 3000 k. Astrophys. J. 326, 509–515.

Borysow, J., Trafton, L., Frommhold, L., Birnbaum, G., 1985. Modeling of pressure-induced far-infrared absorption-spectra: molecular-hydrogen pairs. Astrophys. J. 296, 644–654.

Chamberlain, J.W., Hunten, D.M., 1987. Theory of planetary atmospheres. An introduction to their physics and chemistry. Number 36 in International Geophysics Series, Academic Press Inc., Orlando. 2nd edition.

Davis, E.J., 2006. A history and state-of-the-art of accommodation coefficients. Atmospheric Research 82, 561–578.

de Graauw, T., Helmich, F.P., Phillips, T.G., Stutzki, J., Caux, E., Whyborn, N.D., Dieleman, P., Roelfsema, P.R., Aarts, H., Assendorp, R., Bachiller, R., Baechtold, W., Barcia, A., Beintema, D.A., Belitsky, V., Benz, A.O., Bieber, R., Boogert, A., Borys, C., Bumble, B., Caïs, P., Caris, M., Cerulli-Irelli, P., Chattopadhyay, G., Cherednichenko, S., Ciechanowicz, M., Coeur-Joly, O., Comito, C., Cros, A., de Jonge, A., de Lange, G., Delforges, B., Delorme, Y., den Boggende, T., Desbat, J.M., Diez-González, C., di Giorgio, A.M., Dubbeldam, L., Edwards, K., Eggens, M., Erickson, N., Evers, J., Fich, M., Finn, T., Franke, B., Gaier, T., Gal, C., Gao, J.R., Gallego, J.D., Gauffre, S., Gill, J.J., Glenz, S., Golstein, H., Goulooze, H., Gunsing, T., Güsten, R., Hartogh, P., Hatch, W.A., Higgins, R., Honingh, E.C., Huisman, R., Jackson, B.D., Jacobs, H., Jacobs, K., Jarchow, C., Javadi, H., Jellema, W., Justen, M., Karpov, A., Kasemann, C., Kawamura, J., Keizer, G., Kester, D., Klapwijk, T.M., Klein, T., Kollberg, E., Kooi, J., Kooiman, P.P., Kopf, B., Krause, M., Krieg, J.M., Kramer, C., Kruizenga, B., Kuhn, T., Laauwen, W., Lai, R., Larsson, B.,

Leduc, H.G., Leinz, C., Lin, R.H., Liseau, R., Liu, G.S., Loose, A., López-Fernandez, I., Lord, S., Luinge, W., Marston, A., Martín-Pintado, J., Maestrini, A., Maiwald, F.W., McCoey, C., Mehdi, I., Megej, A., Melchior, M., Meinsma, L., Merkel, H., Michalska, M., Monstein, C., Moratschke, D., Morris, P., Muller, H., Murphy, J.A., Naber, A., Natale, E., Nowosielski, W., Nuzzolo, F., Olberg, M., Olbrich, M., Orfei, R., Orleanski, P., Ossenkopf, V., Peacock, T., Pearson, J.C., Peron, I., Phillip-May, S., Piazzo, L., Planesas, P., Rataj, M., Ravera, L., Risacher, C., Salez, M., Samoska, L.A., Saraceno, P., Schieder, R., Schlecht, E., Schlöder, F., Schmülling, F., Schultz, M., Schuster, K., Siebertz, O., Smit, H., Szczerba, R., Shipman, R., Steinmetz, E., Stern, J.A., Stokroos, M., Teipen, R., Teyssier, D., Tils, T., Trappe, N., van Baaren, C., van Leeuwen, B.J., van de Stadt, H., Visser, H., Wildeman, K.J., Wafelbakker, C.K., Ward, J.S., Wesselius, P., Wild, W., Wulff, S., Wunsch, H.J., Tielens, X., Zaal, P., Zirath, H., Zmuidzinas, J., Zwart, F., 2010. The Herschel-Heterodyne Instrument for the Far-Infrared (HIFI). Astron. Astrophys. 518, L6.

Fast, K., Kostiuk, T., Romani, P., Espenak, F., Hewagama, T., Betz, A., Boreiko, R., Livengood, T., 2002. Temporal Behavior of Stratospheric Ammonia Abundance and Temperature Following the SL9 Impacts. Icarus 156, 485–497.

Fegley, B., Lodders, K., 1994. Chemical models of the deep atmospheres of Jupiter and Saturn. Icarus 110, 117–154.

Feuchtgruber, H., Lellouch, E., Encrenaz, T., Bezard, B., Coustenis, A., Drossart, P., Salama, A., de Graauw, T., Davis, G.R., 1999. Oxygen in

the stratospheres of the giant planets and Titan, in: Cox, P., Kessler, M. (Eds.), The Universe as Seen by ISO, pp. 133–136.

Feuchtgruber, H., Lellouch, E., de Graauw, T., Bézard, B., Encrenaz, T., Griffin, M., 1997. External supply of oxygen to the atmospheres of the giant planets. Nature 389, 159–162.

Flasar, F.M., Kunde, V.G., Abbas, M.M., Achterberg, R.K., Ade, P., Barucci, A., Bézard, B., Bjoraker, G.L., Brasunas, J.C., Calcutt, S., Carlson, R., Esarsky, C.J.C., Conrath, B.J., Coradini, A., Courtin, R., Coustenis, A., Edberg, S., Edgington, S., Ferrari, C., Fouchet, T., Gautier, D., Gierasch, P.J., Grossman, K., Irwin, P., Jennings, D.E., Lellouch, E., Mamoutkine, A.A., Marten, A., Meyer, J.P., Nixon, C.A., Orton, G.S., Owen, T.C., Pearl, J.C., Prange, R., Raulin, F., Read, P.L., Romani, P.N., Samuelson, R.E., Segura, M.E., Showalter, M.R., Simon-Miller, A.A., Smith, M.D., Spencer, J.R., Spilker, L.J., Taylor, F.W., 2004. Exploring the Saturn system in the thermal infrared: The Composite Infrared Spectrometer. Space Sci. Rev. 115, 169–297.

Fletcher, L.N., Orton, G.S., de Pater, I., Edwards, M.L., Yanamandra-Fisher, P.A., Hammel, H.B., Lisse, C.M., Fisher, B.M., 2011. The aftermath of the July 2009 impact on Jupiter: Ammonia, temperatures and particulates from Gemini thermal infrared spectroscopy. Icarus 211, 568–586.

Fletcher, L.N., Orton, G.S., Teanby, N.A., Irwin, P.G.J., 2009. Phosphine on Jupiter and Saturn from Cassini/CIRS. Icarus 202, 543–564.

Fletcher, L.N., Swinyard, B., Salji, C., Polehampton, E., Fulton, T., Sidher,

S., Lellouch, E., Moreno, R., Orton, G., Cavalié, T., Courtin, R., Rengel, M., Sagawa, H., Davis, G.R., Hartogh, P., Naylor, D., Walker, H., Lim, T., 2012. Sub-millimetre spectroscopy of Saturn's trace gases from Herschel/SPIRE. Astron. Astrophys. 539, A44.

Fouchet, T., Orton, G., Irwin, P.G.J., Calcutt, S.B., Nixon, C.A., 2004. Upper limits on hydrogen halides in Jupiter from Cassini/CIRS observations. Icarus 170, 237–241.

Goody, R.M., Yung, Y.L., 1989. Atmospheric Radiation: Theoretical Basis. Oxford University Press, Oxford. 2nd edition.

Grevesse, N., Asplund, M., Sauval, A.J., 2007. The Solar Chemical Composition. Space Sci. Rev. 130, 105–114.

Gubbins, D., 2004. Time series analysis and inverse theory for geophysicists. Cambridge Univ. Press, Cambridge UK.

HIFI Observers' Manual, 2011. HERSCHEL-HSC-DOC-0784. Version 2.4, http://herschel.esac.esa.int/Docs/HIFI/pdf/hifi_om.pdf.

Irwin, P., Teanby, N., de Kok, R., Fletcher, L., Howett, C., Tsang, C., Wilson, C., Calcutt, S., Nixon, C., Parrish, P., 2008. The NEMESIS planetary atmosphere radiative transfer and retrieval tool. J. Quant. Spectro. Rad. Trans. 109, 1136–1150.

Kerola, D.X., Larson, H.P., Tomasko, M.G., 1997. Analysis of the near-IR spectrum of Saturn: a comprehensive radiative transfer model of its middle and upper troposphere. Icarus 127, 190–212.

Küppers, M., Schneider, N.M., 2000. Discovery of chlorine in the Io torus. Geophys. Res. Lett. 27, 513–516.

Lacis, A.A., Oinas, V., 1991. A description of the correlated k distribution method for modeling nongray gaseous absorption, thermal emission, and multiple-scattering in vertically inhomogeneous atmospheres. J. Geophys. Res. 96, 9027–9063.

Lellouch, E., Bézard, B., Moses, J.I., Davis, G.R., Drossart, P., Feuchtgruber, H., Bergin, E.A., Moreno, R., Encrenaz, T., 2002. The Origin of Water Vapor and Carbon Dioxide in Jupiter's Stratosphere. Icarus 159, 112–131.

Li, Y.Q., Zhang, H.Z., Davidovits, P., Jayne, J.T., Kolb, C.E., Worsnop, D.R., 2002. Uptake of HCl(g) and HBr(g) on Ethylene Glycol Surfaces as a Function of Relative Humidity and Temperature. J. Phys. Chem. A 106, 1220–1227.

Moses, J.I., Allen, M., Gladstone, G.R., 1995. Nitrogen and oxygen photochemistry following SL9. Geophys. Res. Lett. 22, 1601–1604.

Niemann, H., Atreya, S., Carignan, G., Donahue, T., Haberman, J., Harpold, D., Hartle, R., Hunten, D., Kasprzak, W., Mahaffy, P., Owen, T., Way, S., 1998. The composition of the Jovian atmosphere as determined by the Galileo probe mass spectrometer. J. Geophys. Res. 103, 22831–22846.

Nixon, C.A., Achterberg, R.K., Romani, P.N., Allen, M., Zhang, X., Teanby, N.A., Irwin, P.G.J., Flasar, F.M., 2010. Abundances of Jupiter's trace hydrocarbons from Voyager and Cassini. Plan. & Space Sci. 58, 1667–1680.

Noll, K.S., 1996. Halogens in the giant planets: upper limits to HBr in Saturn and Jupiter. Icarus 124, 608–615.

Ott, S., 2010. The Herschel Data Processing System - HIPE and Pipelines - Up and Running Since the Start of the Mission, in: Mizumoto, Y., Morita, K.I., Ohishi, M. (Eds.), Astronomical Data Analysis Software and Systems XIX, pp. 139–142.

Press, W.H., Flannery, B.P., Teukolsky, S.A., Vetterling, W.T., 1992. Numerical Recipes. Cambridge Univ. Press, Cambridge UK. 2nd edition.

Roelfsema, P.R., Helmich, F.P., Teyssier, D., Ossenkopf, V., Morris, P., Olberg, M., Shipman, R., Risacher, C., Akyilmaz, M., Assendorp, R., Avruch, I.M., Beintema, D., Biver, N., Boogert, A., Borys, C., Braine, J., Caris, M., Caux, E., Cernicharo, J., Coeur-Joly, O., Comito, C., de Lange, G., Delforge, B., Dieleman, P., Dubbeldam, L., de Graauw, T., Edwards, K., Fich, M., Flederus, F., Gal, C., di Giorgio, A., Herpin, F., Higgins, D.R., Hoac, A., Huisman, R., Jarchow, C., Jellema, W., de Jonge, A., Kester, D., Klein, T., Kooi, J., Kramer, C., Laauwen, W., Larsson, B., Leinz, C., Lord, S., Lorenzani, A., Luinge, W., Marston, A., Martín-Pintado, J., McCoey, C., Melchior, M., Michalska, M., Moreno, R., Müller, H., Nowosielski, W., Okada, Y., Orleański, P., Phillips, T.G., Pearson, J., Rabois, D., Ravera, L., Rector, J., Rengel, M., Sagawa, H., Salomons, W., Sánchez-Suárez, E., Schieder, R., Schlöder, F., Schmülling, F., Soldati, M., Stutzki, J., Thomas, B., Tielens, A.G.G.M., Vastel, C., Wildeman, K., Xie, Q., Xilouris, M., Wafelbakker, C., Whyborn, N., Zaal, P., Bell, T., Bjerkeli, P., De Beck, E., Cavalié, T., Crockett, N.R., Hily-Blant, P.,

Kama, M., Kaminski, T., Leflóch, B., Lombaert, R., de Luca, M., Makai, Z., Marseille, M., Nagy, Z., Pacheco, S., van der Wiel, M.H.D., Wang, S., Yıldız, U., 2012. In-orbit performance of Herschel-HIFI. Astron. Astrophys. 537, A17.

Rothman, L.S., Jacquemart, D., Barbe, A., Benner, D.C., Birk, M., Brown, L.R., Carleer, M.R., Chackerian, C., Chance, K., Coudert, L.H., Dana, V., Devi, V.M., Flaud, J.M., Gamache, R.R., Goldman, A., Hartmann, J.M., Jucks, K.W., Maki, A.G., Mandin, J.Y., Massie, S.T., Orphal, J., Perrin, A., Rinsland, C.P., Smith, M.A.H., Tennyson, J., Tolchenov, R.N., Toth, R.A., Vander Auwera, J., Varanasi, P., Wagner, G., 2005. The HITRAN 2004 molecular spectroscopic database. J. Quant. Spectro. Rad. Trans. 96, 139–204.

Rudich, Y., 2003. Laboratory perspectives on the chemical transformations of organic matter in atmospheric particles. Chem. Rev. 103, 5097–5124.

Schweitzer, F., Mirabel, P., George, C., 2000. Uptake of Hydrogen Halides by Water Droplets. J. Phys.l Chem. A 104, 72–76.

Seiff, A., Kirk, D.B., Knight, T.C.D., Mihalov, J.D., Blanchard, R.C., Young, R.E., Schubert, G., von Zahn, U., Lehmacher, G., Milos, F.S., Wang, J., 1996. Structure of the Atmosphere of Jupiter: Galileo Probe Measurements. Science 272, 844–845.

Showman, A.P., 2001. Hydrogen halides on Jupiter and Saturn. Icarus 152, 140–150.

Tabazadeh, A., Turco, R.P., 1993. Stratospheric chlorine injection by volcanic eruptions - HCl scavenging and implications for ozone. Science 260, 1082–1086.

Tabor, D., 1993. Gases, liquids and solids: and other states of matter. Cambridge University Press, Cambridge. 3rd edition.

Teanby, N.A., Fletcher, L.N., Irwin, P.G.J., Fouchet, T., Orton, G.S., 2006. New upper limits for hydrogen halides on Saturn derived from Cassini-CIRS data. Icarus 185, 466–475.

Teanby, N.A., Irwin, P.G.J., 2013. An External Origin for Carbon Monoxide on Uranus from Herschel/SPIRE? Astrophys. J. 775, L49.

Teanby, N.A., Irwin, P.G.J., Nixon, C.A., Courtin, R., Swinyard, B.M., Moreno, R., Lellouch, E., Rengel, M., Hartogh, P., 2013. Constraints on Titan's middle atmosphere ammonia abundance from Herschel/SPIRE sub-millimetre spectra. Plan. & Space Sci. 75, 136–147.

Weisstein, E.W., Serabyn, E., 1996. Submillimeter line search in Jupiter and Saturn. Icarus 123, 23–36.

Wilson, T.L., Rohlfs, K., Hüttemeister, S., 2009. Tools of Radio Astronomy. Springer-Verlag, Berlin. 5th edition.

Woan, G., 2003. The Cambridge Handbook of Physics Formulas. Cambridge University Press, Cambridge.

Wong, M.H., Mahaffy, P.R., Atreya, S.K., Niemann, H.B., Owen, T.C., 2004.

Updated Galileo probe mass spectrometer measurements of carbon, oxygen, nitrogen, and sulfur on Jupiter. Icarus 171, 153–170.

Zhang, H.Z., Li, Y.Q., Davidovits, P., Williams, L.R., Jayne, J.T., Kolb, C.E., Worsnop, D.R., 2003. Uptake of Gas-Phase Species by 1-Octanol. 2. Uptake of Hydrogen Halides and Acetic Acid as a Function of Relative Humidity and Temperature. J. Phys. Chem. A 107, 6398–6407.

Observation	Band	ID	Date	Start (UT)	Dur. (s)	WBS Freq. Range (GHz)			Δf (MHz)	θ_H (°N)	Diam (")	Range (AU)	e (°)	DFWHM (MHz)
1342266402	1	B1A	07/03/2013	19:10:22	4640	624.2270	-	628.3560	0.5	3.05	38.29	5.149	39.86	35.39
1342266403	1	B1B	07/03/2013	20:00:22	4520	624.1505	-	628.2795	0.5	3.05	38.29	5.149	39.86	35.39
1342266404	1	B1C	07/03/2013	20:50:22	4440	624.3375	-	628.4665	0.5	3.05	38.28	5.150	39.86	35.39
1342266597	7	B7B	28/02/2013	02:10:42	2914	1875.5715	-	1878.1340	0.5	3.07	39.25	5.023	15.52	39.65
1342266598	7	B7b	28/02/2013	03:30:00	2914	1875.4975	-	1878.0600	0.5	3.07	39.24	5.024	15.52	39.65
1342266599	7	B7C	28/02/2013	04:47:18	2914	1875.6795	-	1878.2420	0.5	3.07	39.24	5.025	15.52	39.65

Table 1: Observation summary. The total integration time in each of the two HCl bands was split into three observation blocks. For each observation, both horizontal and vertical polarisations were measured. Parameters are: Dur., observation block duration; Δf, WBS frequency spacing; θ_H, sub-Herschel latitude; Diam, angular diameter of Jupiter; Range, Herschel-Jupiter distance; e, weighted mean emission angle; and DFWM, equivalent doppler FWHM of spectral lines.

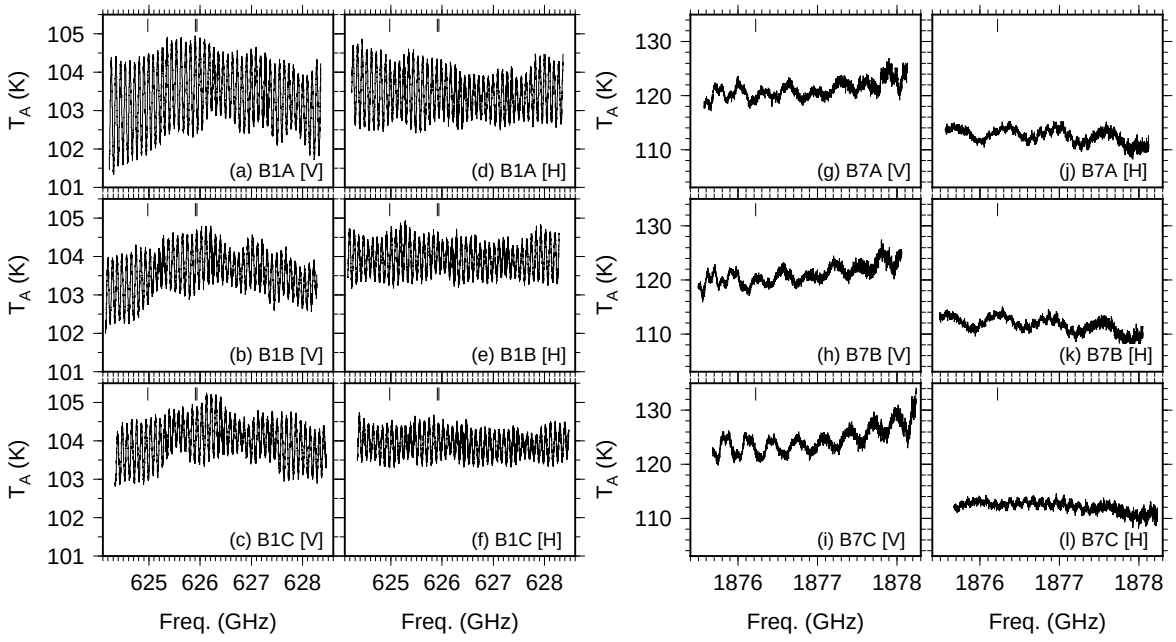

Figure 1: Antenna temperature spectra. Level 2 reduced Herschel/HIFI pipeline spectra for band 1 (a–f) and band 7 (g–l). [H] and [V] indicate horizontal and vertical polarisations respectively. All spectra suffer from standing wave interference: predominantly with periods of ∼100 MHz in band 1 and ∼320 MHz in band 7.

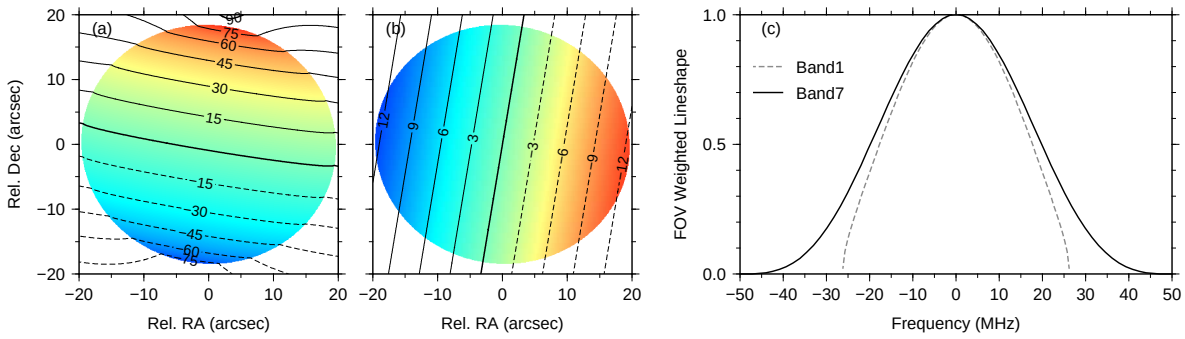

Figure 2: Effective doppler broadened lineshapes. (a) Orientation of Jupiter as viewed from Herschel during the HIFI observations. Contours show planetocentric latitude. (b) Line-of-sight velocity in $\mathrm{km\,s^{-1}}$, where positive values are towards Herschel (blue-shifted). (c) Doppler broadened lineshapes, incorporating weighting by Herschel's Airy disc for band 1 (626.25 GHz) and band 7 (1876.75 GHz).

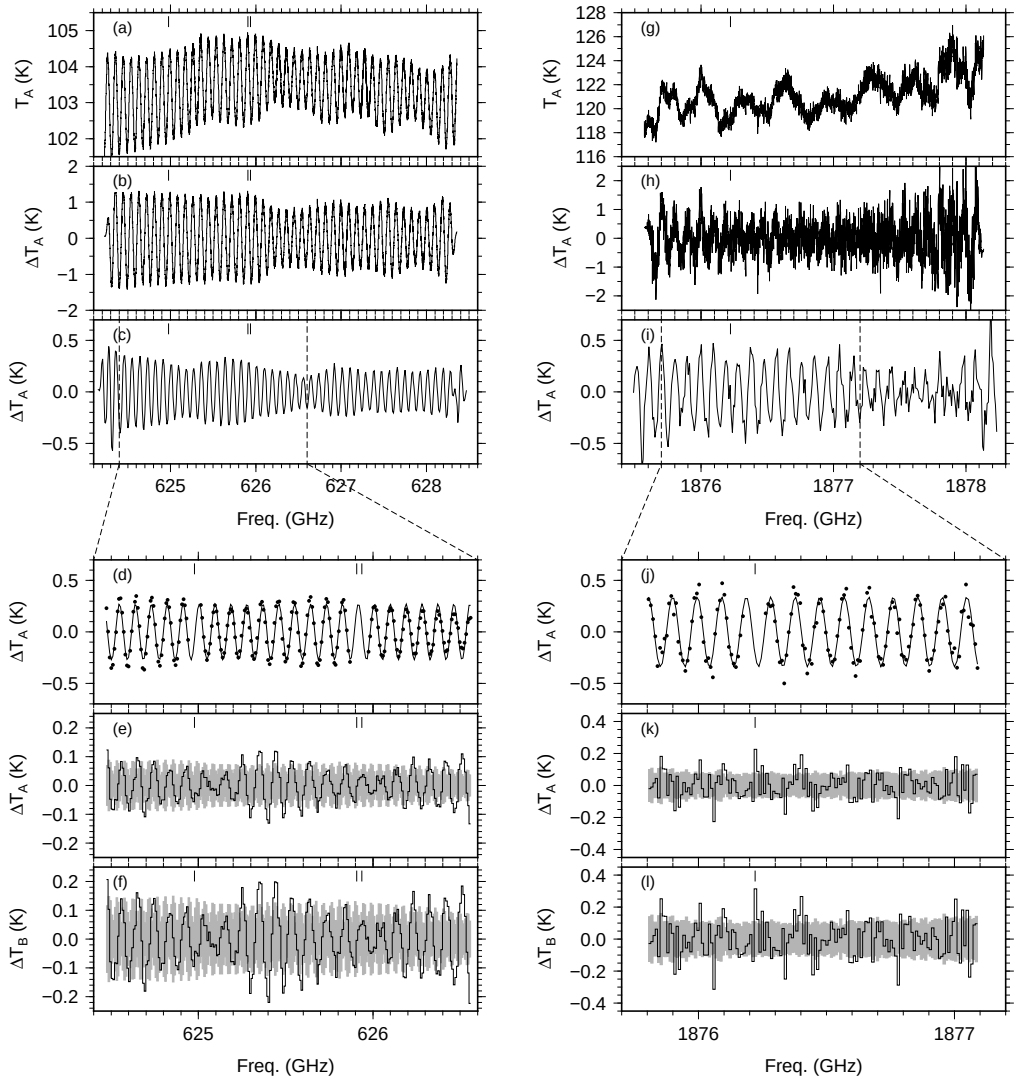

Figure 3: Data processing to reduce standing wave interference. (a) A single band 1 observation (vertical polarisation). (b) A single band 1 observation after application of a 200 MHz 4 pole high-pass Butterworth filter. (c) All six filtered horizontal and vertical polarisation observations for band 1 averaged with 9 MHz width bins to reduce random noise. (d) Zoom of a 2.2 GHz spectral segment, with the HCl line positions masked out, and a single frequency sine wave fitted to represent the standing wave contribution. (e) Residual spectrum after removal of the fitted sine wave. (f) Antenna temperature converted to brightness temperature. (g–l) The same procedure illustrated for band 7, which is identical to the process for band 1 except that the sine wave is fitted to a 1.5 GHz segment in this case. Vertical dashes near the top of each plot show the positions of HCl spectral lines. Grey envelopes indicate 1-σ errorbars.

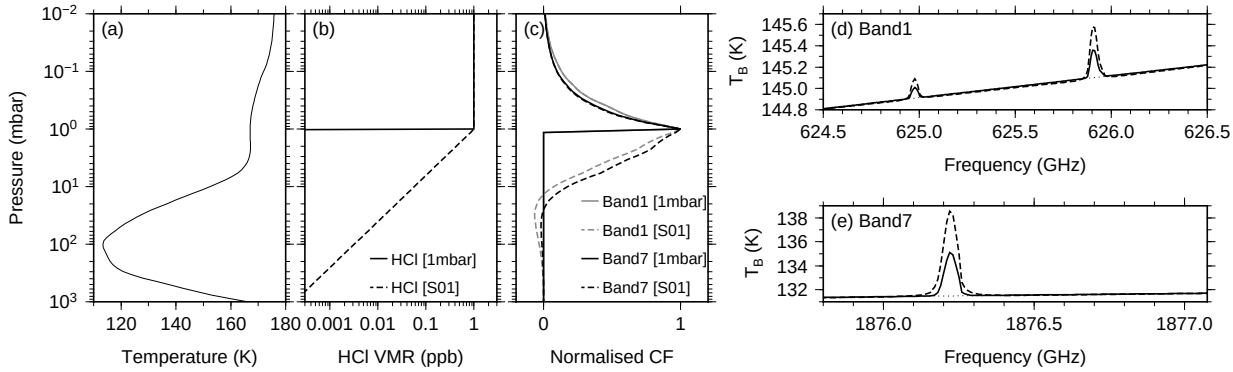

Figure 4: Predicted spectra for 1 ppb HCl at 1 mbar. (a) Assumed Jupiter pressure-temperature profile. (b) The two reference HCl profiles: [1 mbar] HCl uniformly mixed above 1 mbar and zero for higher pressures (solid lines); [S01] as [1 mbar] but with HCl abundances for higher pressures from the 1D diffusion model in Showman (2001) (dashed lines). (c) contribution functions at the HCl line centre for each of the reference profiles. Peak sensitivity of these observations is around 1 mbar with these profiles. (d,e) Synthetic spectra for band 1 and band 7 using the reference profiles and incorporating the doppler-broadened lineshape.

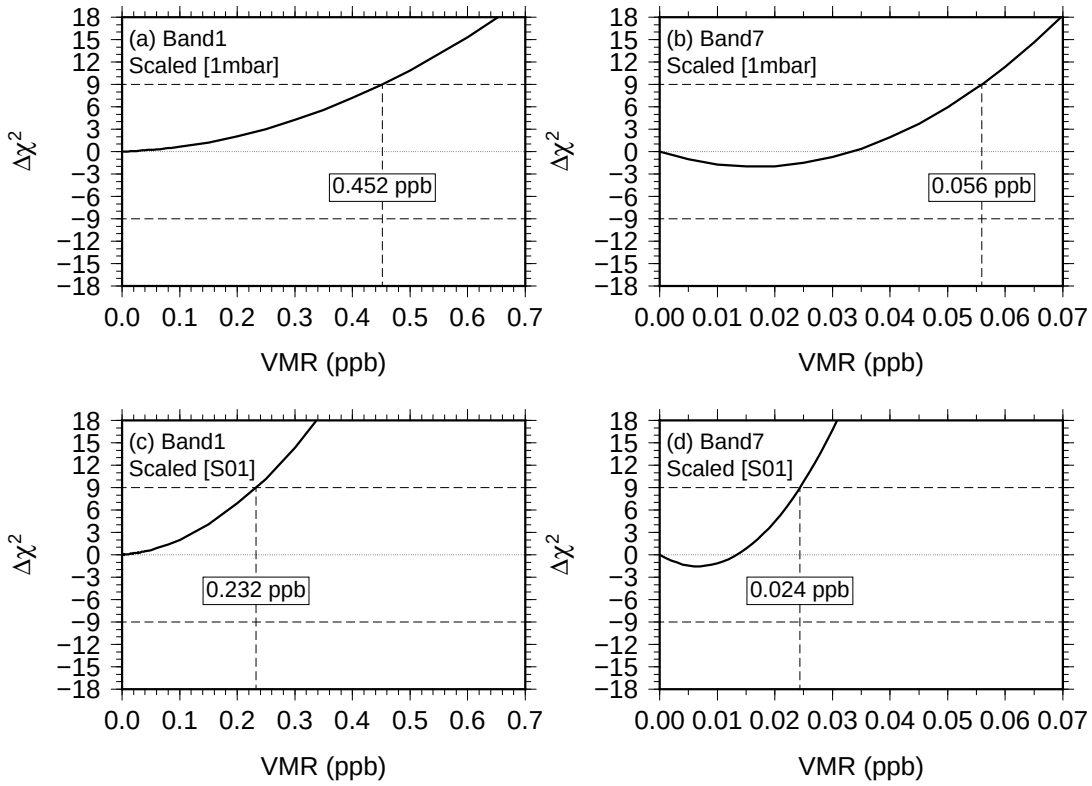

Figure 5: Variation of $\Delta\chi^2$ misfit as a function of HCl volume mixing ratio (VMR) at 1 mbar. (a,b) Band 1/band 7 with a scaled [1 mbar] reference profile. (c,d) Band 1/band 7 with a scaled [S01] reference profile. Dashed line at $\Delta\chi^2$=-9 shows the requirement for a 3-σ detection, which is not satisfied for either band 1 or band 7 spectra, indicating that HCl is not detected. Upper dashed line at $\Delta\chi^2$=+9 shows requirement for a 3-σ upper limit. VMRs in boxes give the upper limits for each profile and spectral band. Band 7 provides the most stringent constraints on HCl abundance.

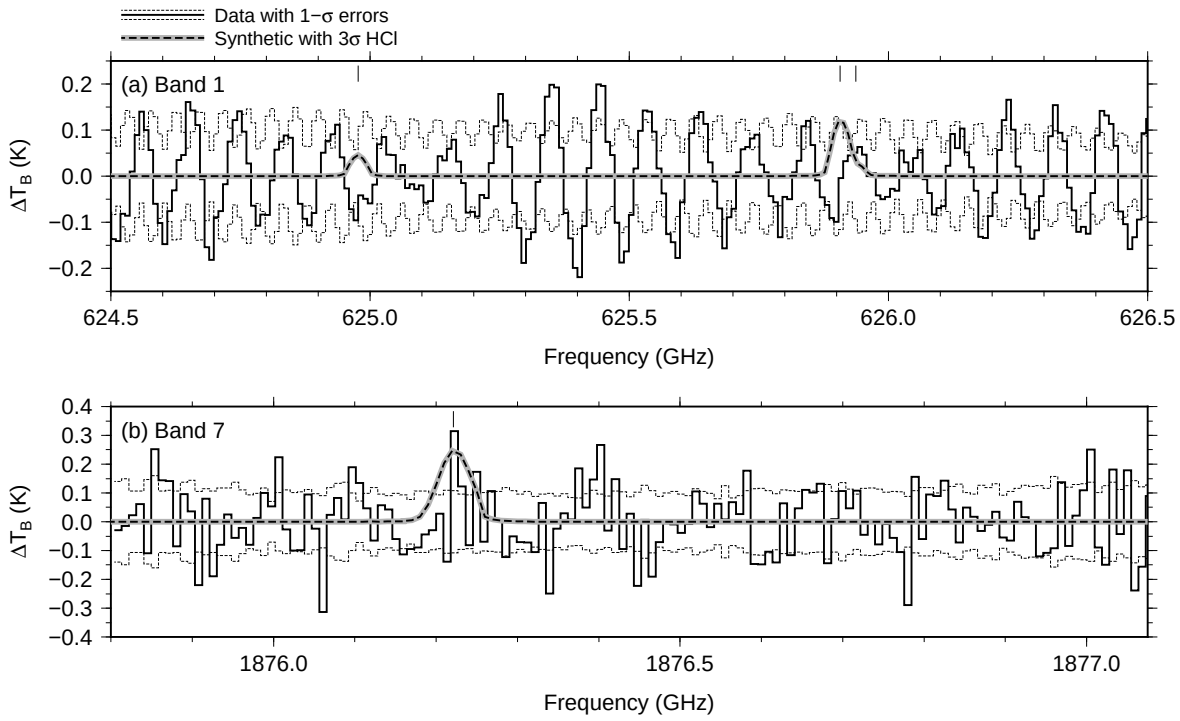

Figure 6: Synthetic spectra with upper limit abundances compared to observations. (a) Band 1 observation compared to a synthetic with 0.452 ppb HCl at 1 mbar using the [1 mbar] profile. (b) Band 7 observation compared to a synthetic with 0.056 ppb HCl at 1 mbar using the [1 mbar] profile. No significant HCl spectral features are visible in either set of observations. For band 7, there is a single bin displaying a high brightness temperature in the position of a HCl spectral line. However, the lineshape is incorrect, its height is comparable to other noise features, and the χ^2 analysis shows this not to be significant. Therefore, we regard this feature as spurious and attribute it to noise.

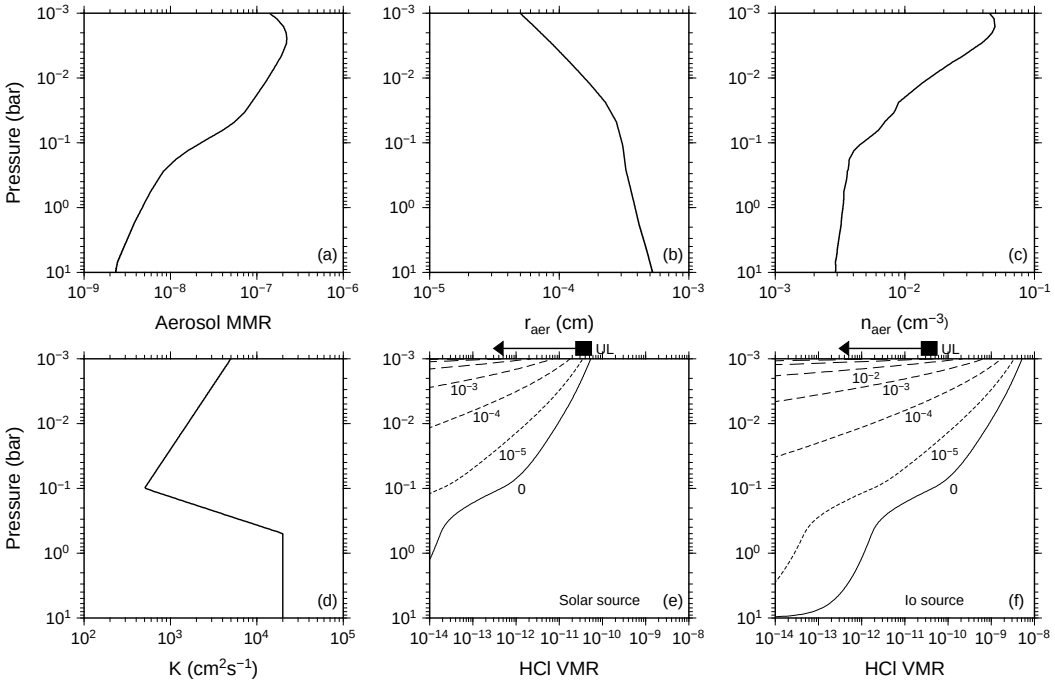

Figure 7: Diffusion model of HCl mixing and scavenging. (a) Aerosol mass mixing ratio (grammes of aerosol per gramme of atmosphere) from Banfield et al. (1998). (b) Aerosol radii profile from Banfield et al. (1998). (c) Number density of aerosols in the model. (d) Eddy diffusion profile used in the model (taken from Showman (2001)). (e) Predicted HCl profile for an external Cl flux of 2.8×10^3 molecules/cm^2/s injected at 1 mbar, appropriate for a solar composition source (such as comets). Labelled lines indicate predicted HCl profiles for HCl-aerosol scavenging accommodation coefficients of γ=0, 10^{-5}, 10^{-4}, 10^{-3}, 10^{-2}, 0.1, and 1. Black box with arrow at 1 mbar indicates upper limits derived from our Herschel/HIFI observations. Any value of γ over 10^{-4}–10^{-5} gives a result consistent with our observations. (f) as for (e) except for an external Cl flux of 2.7×10^5 molecules/cm^2/s, appropriate for a Cl and O source from Io. A value of γ of at least 0.1 is required to be consistent with our observations, which is most probably too high given current lab measurements with organic compounds.

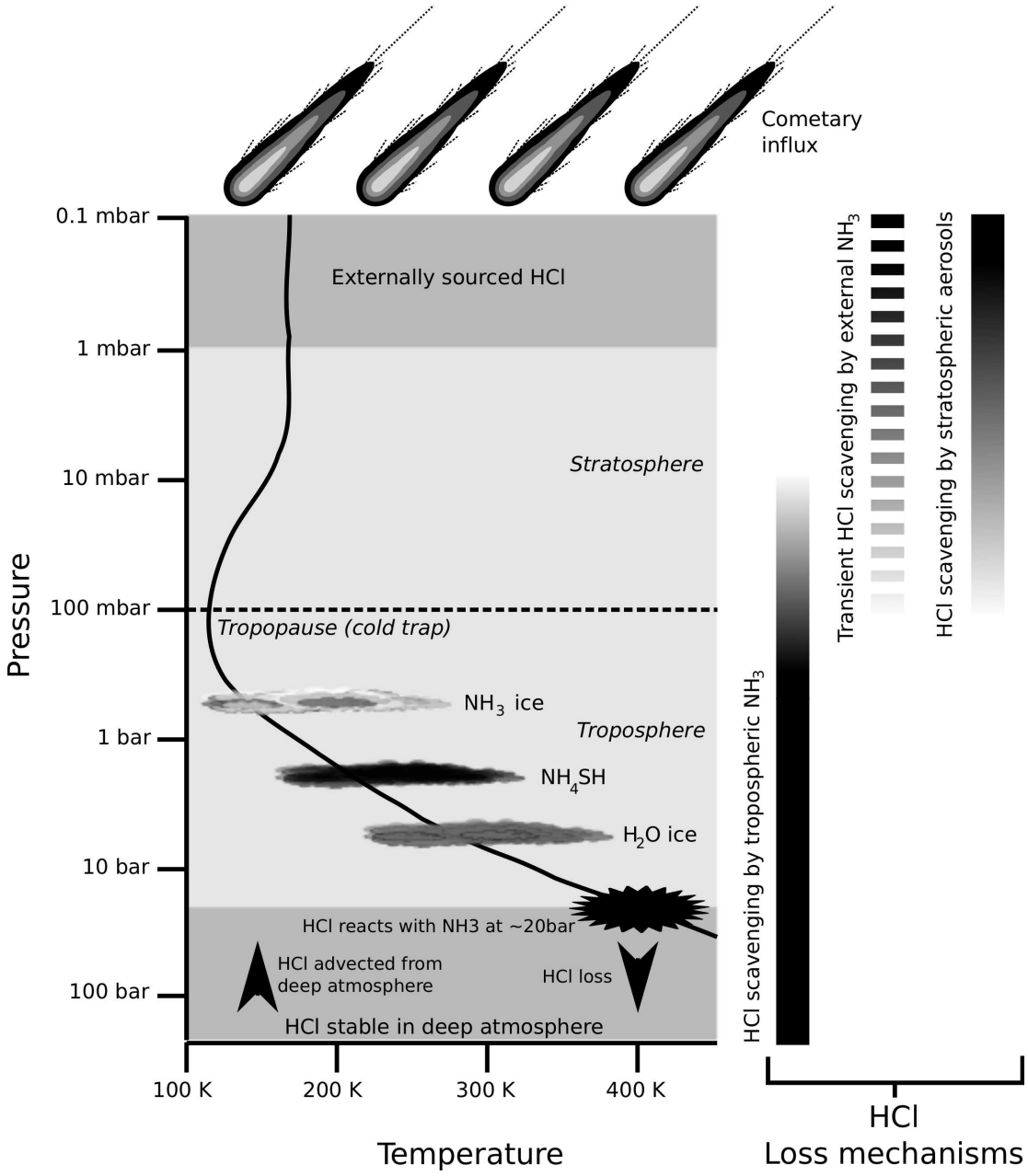

Figure 8: Schematic of Jupiter's chlorine cycle. Deep HCl lofted by convection becomes unstable at temperatures of 400K or less and reacts with NH_3 to form NH_4Cl and is recycled back into the deep atmosphere. Any residual HCl from the deep interior is scavenged by tropospheric NH_3 up until pressure levels of around 10 mbar, where all NH_3 will have been effectively removed by the tropopause cold trap and photolysis. Above the 1 mbar pressure level, externally sourced Cl forms HCl, but is most likely scavenged by stratospheric aerosols (a continuous/global process indicated with solid vertical bar) and externally sourced or impact plume excavated NH_3 (a transient/local process indicated by broken vertical bar).